International Journal of Heat and Mass Transfer 181 (2021) 121835

Contents lists available at ScienceDirect

International Journal of Heat and Mass Transfer

journal homepage: www.elsevier.com/locate/hmt

On the mechanism of onset of significant void in subcooled flow boiling

Tomio Okawa

Department of Mechanical & Intelligent Systems Engineering, The University of Electro-Communications, 1-5-1, Chofugaoka, Chofu-shi, Tokyo 182-8585, Japan

ARTICLE INFO

Article history:
Received 7 June 2021
Revised 25 July 2021
Accepted 9 August 2021
Available online 20 August 2021

Keywords:
Subcooled flow boiling
Onset of significant void (OSV)
Net vapor generation (NVG)
Mechanistic modelling
Bubble coalescence
Heat flux partitioning

ABSTRACT

Theoretical investigation was carried out for a possible mechanism of the onset of significant void (OSV) or net vapor generation (NVG) in subcooled flow boiling. Based on available knowledge on the two-phase flow regime transition from bubbly to slug flows, it was postulated that bubble coalescence is intensified substantially when the local void fraction near the heated wall exceeds a critical value. It was discussed that this can be a main cause of a rapid increase in the cross-sectional area-averaged void faction since the condensation rate decreases suddenly due to a sudden decrease in the interfacial area of vapor bubbles. It was demonstrated that if the vaporization rate on the heat transfer surface is evaluated using a reliable wall heat transfer correlation, the OSV conditions calculated by the present model agree with those by a widely-used empirical correlation well.

1. Introduction

When wall heat flux is applied to the subcooled liquid flowing in a tube, both the liquid and wall temperatures increase gradually in the axial direction and nucleate boiling is commenced at the position where the wall superheat becomes high enough. This phenomenon is referred to as the onset of nucleate boiling (ONB). In the region downstream of the position of ONB (PONB), the cross-sectional area-averaged void fraction is positive since vapor bubbles are present. In a certain region just downstream of PONB, however, the liquid subcooling is still so high that the void fraction is maintained at a low value [1–3]. Thus, the void fraction in this region is neglected in many practical applications [2]. At the point where the liquid subcooling becomes sufficiently low, a rapid increase in the void fraction is permitted eventually. This phenomenon is referred to as the onset of significant void (OSV) or the net vapor generation (NVG). Thus, the void fraction starts to rise rather discontinuously at the point of OSV (POSV). The void fraction in the region downstream of POSV is appreciable and should normally be taken into consideration although the bulk temperature does not yet reach the saturation temperature [2].

The ability to calculate the bulk liquid subcooling at POSV accurately is the most important element in predicting the axial void fraction profile in the subcooled flow boiling region [2]. In addition, the void fraction profile in the subcooled boiling region is of significant importance in the design of light-water reactors since it influences the pressure drop, two-phase flow instability, and fuel burnup. Thus, many correlations have been developed so far for the critical liquid subcooling to cause OSV in subcooled flow boiling as reviewed extensively by Cai et al. [4]. These correlations clarified important parametric trends such as an increase in the critical subcooling with an increase in the heat flux and a decrease in the mass flux [5–8]. Among available correlations, the simple empirical correlation developed by Saha and Zuber [9] provides particularly good predictions of the critical subcooling at OSV. It has been reported that their correlation predicts the critical subcooling within the error range of about ±25% in wide ranges of thermal-hydraulic conditions [4,9,10].

In contrast to the good prediction capability of the critical subcooling, the mechanism to cause OSV has not been understood sufficiently. It is often supposed that bubbles adhere to the heated wall in Region I (the region between PONB and POSV) and they are ejected from the wall in Region II (the region downstream of POSV) [1–3]. Based on this concept, Levy [11] assumed that the sum of the buoyant force and the frictional force to remove the bubble is balanced with the surface tension force to hold it at POSV to develop a mechanistic model for the critical subcooling. Dix [12] however observed experimentally that the bubbles are present only near the wall but do not adhere to the wall even in Region I. To resolve this contradiction, Dix presumed that the bubbles travel in the narrow bubble layer close to the wall in Region I and they are ejected into the bulk liquid in Region II. It was further assumed that the bubble layer formed on the heated wall should

https://doi.org/10.1016/j.ijheatmasstransfer.2021.121835
0017-9310/

Nomenclature

A	cross-sectional area
$C_1 - C_4$	model constants
C_D	drag coefficient
c_p	specific heat at constant pressure
D	flow channel diameter
D^*	diameter ratio ($= D/d_B$)
d_B	bubble diameter
Eo	Eötvös number ($= g\Delta\rho {d_B}^2/\sigma$)
F	enhancement factor of force-convection heat transfer
G	mass flux
G^*	parameter related to inertia ratio of bulk liquid to micro convection ($= (G\Delta h_{VAP}/q_W)(\rho_L/\rho_V)^n$)
g	gravitational acceleration
h	heat transfer coefficient
h^*	heat transfer coefficient ratio ($= Sh_{NB}/h_{CON}$)
k	thermal conductivity
n	model constant
P	pressure
P_H	heated perimeter
Pe	Peclet number ($= GDc_{pL}/k_L$)
Pr	Prandtl number
q	heat flux
q^*	dimensionless heat flux (Reynolds number of micro convection) ($= \rho_L q_W d_B/\rho_V \Delta h_{VAP} \mu_L$)
Re	Reynolds number
S	suppression factor of nucleate heat transfer
St	Stanton number ($= q_W/Gc_{pL}\Delta T_{SUB}$)
t	time
u	velocity
u_R	bubble velocity relative to liquid
z	axial coordinate

Greek letters

α	void fraction
σ	surface tension
Δh_{VAP}	latent heat of vaporization
Δp_W	increase of saturation pressure corresponding to ΔT_W
ΔT_{SUB}	liquid subcooling
ΔT_W	wall superheat
Δz	length of control volume
$\Delta\theta_{SUB}$	dimensionless liquid subcooling ($= c_{pL}\Delta T_{SUB}/\Delta h_{VAP}$)
$\Delta\theta_W$	dimensionless wall super heat ($= c_{pL}\Delta T_W/\Delta h_{VAP}$)
$\Delta\rho$	density difference
μ	viscosity
ρ	density
ρ^*	density ratio ($= \rho_L/\rho_V$)
σ	surface tension

Subscripts

B	bubble
BL	bubble layer
C	critical
CON	condensation
FC	forced convection
H	hydrodynamically controlled region
L	liquid
NB	nucleate boiling
PUMP	pumping effect by nucleation
T	thermally controlled region
V	vapor
VAP	vaporization
W	wal

be thick enough for the bubble ejection to occur to develop a correlation for the OSV condition.

If the bubbles adhere to the wall and their size is not very large, the situation is so-called wall voidage and the void fraction at the center of the flow channel is zero. On the other hand, if the bubbles are ejected from the wall, there is a chance that the void fraction is positive even at the center of the flow channel. This would be the main reason why the bubble departure is regarded as the initiating event of OSV. It should however be borne in mind that the local liquid subcooling is higher in the bulk region than in the wall region. Thus, the bubble ejection would contribute to the decrease of the void fraction rather than the increase of it since the bubble condensation is enhanced by the rise of local subcooling around the bubbles. Migration of bubbles to the bulk region may be regarded as the consequence rather than the cause of OSV. In addition, more recent experimental observations showed that the bubble migration toward the bulk liquid occurs even just downstream of PONB [13–15]. It is therefore suggested that available theoretical bases and experimental evidences are not sufficient to regard the bubble detachment from the wall as the main cause of OSV with confidence.

As a different mechanism, Zeitoun [14] and Sun et al. [16] postulated that the vaporization rate is equal to the condensation rate at POSV. This condition would however be true at any point within Region I where the void fraction is maintained low. Rather, it would appear that POSV should be defined as the point where this condition is broken.

Saha and Zuber [9] found that experimental data of the critical subcooling can be collapsed using two empirical correlations depending on the mass flux. The prediction capability of their methodology is excellent and used as the base in several later correlations [17,18]. Based on this result, Saha and Zuber interpreted their correlations to discuss that OSV is caused by the bubble detachment in the high mass flux condition and further reduction of subcooling is required for the bubbles to migrate toward the bulk liquid in the low mass flux condition. This implies that OSV is induced by the hydrodynamically and thermally mechanisms in the high and low mass flux conditions, respectively. Thus, Saha and Zuber referred the two conditions as the hydrodynamically and thermally controlled regions, respectively. However, since their correlations were derived empirically, quantitative investigation would be necessary to confirm the validity of their interpretations.

The above literature survey and discussion show that although available correlations have the capability to calculate the critical subcooling at POSV with reasonable accuracy, the mechanism to cause OSV is still not understood sufficiently. It is noted that most of the available correlations were developed using the experimental data accumulated in simple conditions (e.g., round tube, uniform heat flux, steady state, etc.). More complicated situation is however encountered in light-water reactors particularly during accident. Sufficient understanding of the mechanism causing OSV is useful to include the effects of additional factors that can be of importance in light-water reactors such as the channel geometry, axial heat flux distribution, and transients of heat flux and mass flow rate. In view of this, in the present work, a possible mechanism to cause OSV in subcooled flow boiling is investigated theoretically using the mass conservation equation of the one-dimensional two-fluid model to derive a mechanistic model for OSV. Since good prediction performance of Saha and Zuber's correlation in wide ranges of thermal-hydraulic conditions were

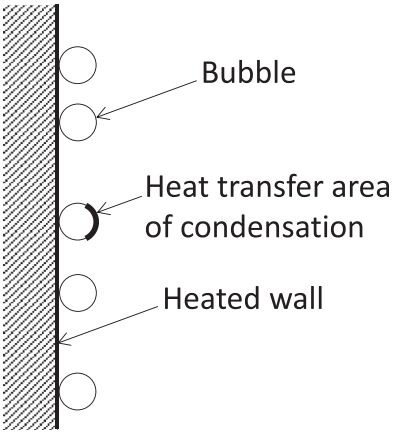

Fig. 1. Schematic diagram of the condensation model.

verified not only by the developers [9] but also by other investigators [4,19], reasonably good agreement with the empirical correlation by Saha and Zuber would be regarded as a sufficiently reliable evidence showing the plausibility of the supposed mechanism of OSV. Hence, the values of the critical subcooling calculated by the present model are compared with those calculated by Saha and Zuber's correlation to explore if the present model is plausible.

2. Modeling of the mechanism of OSV

2.1. Mass conservation equation of vapor phase

The equation used in this work to describe the axial development of the void fraction is the following mass conservation equation for gas phase of the one-dimensional two-fluid model.

$$\frac{\partial}{\partial t}(\alpha\rho_V) + \frac{\partial}{\partial z}(\alpha\rho_V u_V) = \Gamma_{VAP} - \Gamma_{CON} \tag{1}$$

where t is the time, α is the void fraction, ρ is the density, z is the axial coordinate, u is the velocity, Γ is the phase change rate, and the subscripts V, VAP, and CON denote vapor phase, vaporization, and condensation, respectively. Since the void fraction in Region I is low, constant vapor velocity may be assumed. Further assuming steady state and constant vapor density, the above equation is simplified to

$$\frac{d\alpha}{dz} = \frac{\Gamma_{VAP} - \Gamma_{CON}}{\rho_V u_V} \tag{2}$$

For simplicity, it is supposed that axial heat flux profile is uniform. Since the liquid subcooling ΔT_{SUB} decreases linearly under the present circumstances, it is expected that Γ_{VAP} increases and Γ_{CON} decreases gradually in the axial direction and consequently $d\alpha/dz$ also varies gradually in the axial direction. This expectation however conflicts with the experimental fact that $d\alpha/dz$ is nearly zero in Region I and begins to increase suddenly at POSV. To cause the sudden increase of $d\alpha/dz$, Eq. (2) dictates that at least, one of the four quantities Γ_{VAP}, Γ_{CON}, ρ_V and u_V varies suddenly or discontinuously at POSV. The bubble ejection from the wall region to the bulk liquid is commonly regarded as the mechanism to cause OSV [1–3]. If the bubble is ejected into the bulk liquid, however, the local subcooling and liquid velocity around the bubble increase, resulting in the increases of Γ_{CON} and u_V. Eq. (2) therefore suggests that the bubble ejection is the cause of a decrease rather than an increase in the value of $d\alpha/dz$.

2.2. A possible role of bubble coalescence in causing OSV

In gas-liquid two-phase flow, the typical flow pattern at low gas flow rate is the bubbly flow. As the gas flow rate increases, mean distance between bubbles decreases and bubble coalescence is enhanced to cause the flow regime transition from bubbly flow to slug flow [19]. If a large bubble is produced in bubbly flow, small bubbles are captured in the wake region formed behind the large bubble to enhance coalescence [20]. Thus, the flow regime transition to the slug flow is rapid. From a simple geometrical consideration for the bubbles arranged in a tetrahedral lattice pattern, Mishima and Ishii [21] supposed that the transition from bubbly flow to slug flow occurs at $\alpha = 0.3$.

In Region I in subcooled flow boiling, bubbles are present only in the wall region. It would hence be assumed that bubble coalescence is enhanced to form large bubbles when the void fraction in the bubble layer formed in the wall region α_{BL} exceeds the critical void fraction for the flow regime transition to slug flow α_C. The condensation of bubbles occurs at the phase interface. Since the bubble interface per unit bubble volume decreases with an increase in the bubble size, the increase of the bubble size would lead to the decrease of Γ_{CON} and consequently the increase of $d\alpha/dz$ (see Eq. (2)). It is therefore assumed in the present work that OSV occurs when the following criterion is satisfied.

$$\alpha_{BL} = \alpha_C \tag{3}$$

2.3. Calculation method of the void fraction in bubble layer

Since the void fraction α and consequently $d\alpha/dz$ are small in Region I, Eq. (2) may further be simplified to

$$\Gamma_{VAP} = \Gamma_{CON} \tag{4}$$

The vaporization rate is hence nearly balanced with the condensation rate in Region I. This relation is used to estimate the value of the liquid subcooling ΔT_{SUB} when α_{BL} reaches to α_C. In subcooled flow boiling, the wall heat flux q_W is spent for the rise of liquid temperature and vaporization. Using the component spent for vaporization q_{VAP}, Γ_{VAP} is written as

$$\Gamma_{VAP} = \frac{q_{VAP} P_H \Delta z}{\Delta h_{VAP}} \times \frac{1}{A\Delta z} = \frac{q_{VAP} P_H}{\Delta h_{VAP} A} \tag{5}$$

where P_H is the perimeter of the heated area, Δz is the length of the control volume, Δh_{VAP} is the latent heat of vaporization, and A is the cross-sectional area of the flow channel. Denoting the condensation heat transfer coefficient by h_{CON} and the liquid subcooling in the bubble layer by $\Delta T_{SUB,BL}$, Γ_{CON} may be written as

$$\Gamma_{CON} = \frac{h_{CON}\Delta T_{SUB,BL}}{\Delta h_{VAP}} \times C_1 P_H \Delta z \alpha_{BL} \times \frac{1}{A\Delta z} = \frac{C_1 \alpha_{BL} h_{CON} \Delta T_{SUB,BL} P_H}{\Delta h_{VAP} A} \tag{6}$$

As delineated in Fig. 1, it was assumed that all the bubbles are present on the heat wall and the condensation occurs on the bulk side of bubbles. Using the model constant C_1, the heat transfer area of condensation is estimated by $C_1 P_H \Delta z \alpha_{BL}$ in the above equation.

Substituting Eqs. (5) and (6) into Eq. (4) and using Eq. (3), the criterion for OSV is expressed by

$$\alpha_{BL} = \alpha_C = \frac{q_{VAP}}{C_1 C_2 h_{CON} \Delta T_{SUB}} \tag{7}$$

Here, the liquid subcooling in the bubble layer $\Delta T_{SUB,BL}$ is assumed proportional to that of the bulk liquid using the model constant C_2 ($\Delta T_{SUB,BL} = C_2 \Delta T_{SUB}$).

2.4. Closure relationships

Appropriate methods to calculate q_{VAP} and h_{CON} are necessary to estimate the liquid subcooling ΔT_{SUB} at POSV using Eq. (7). Chen [22] expressed the wall heat flux q_W as the sum of the components associated with the forced-convective heat transfer q_{FC}

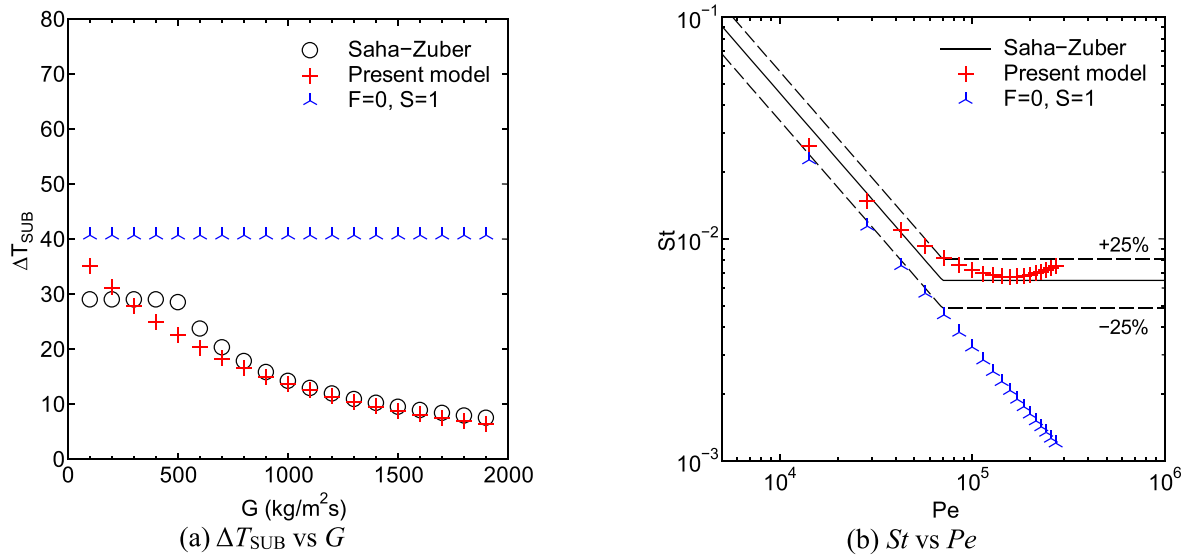

(a) ΔT_{SUB} vs G (b) St vs Pe

Fig. 2. Comparisons of the values of ΔT_{SUB} at OSV calculated by the present and Saha-Zuber correlations in the standard conditions of P, D and q_W.

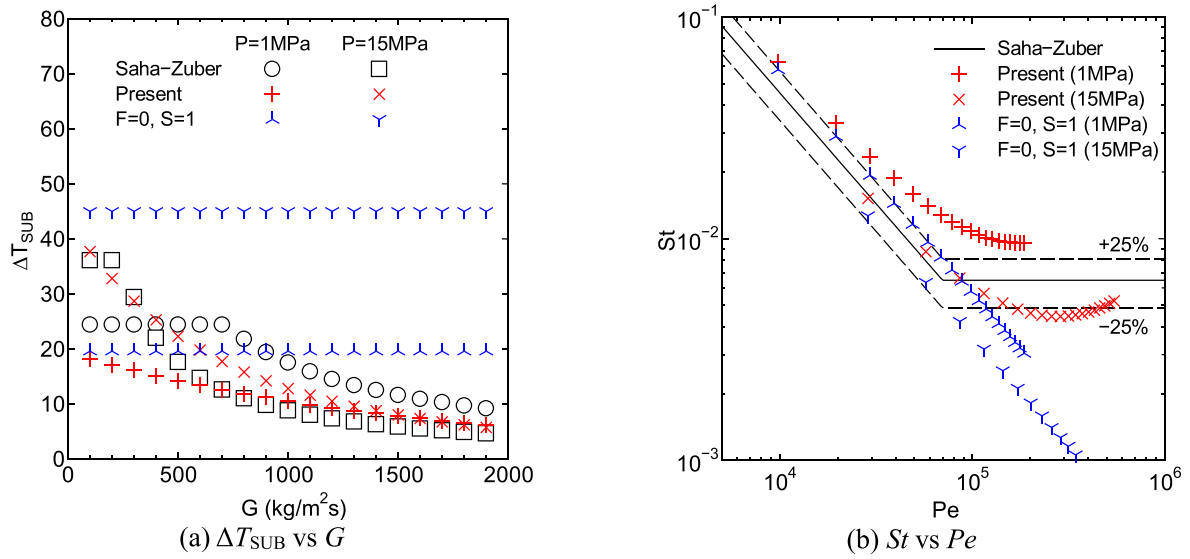

(a) ΔT_{SUB} vs G (b) St vs Pe

Fig. 3. Effect of pressure on the calculated OSV condition.

and nucleate boiling heat transfer q_{NB} as

$$q_W = q_{FC} + q_{NB} \tag{8}$$

Each component is calculated by

$$q_{FC} = Fh_{FC}(\Delta T_W + \Delta T_{SUB}) \tag{9}$$

$$q_{NB} = Sh_{NB}\Delta T_W \tag{10}$$

where h_{FC} and h_{NB} are the heat transfer coefficients for the forced-convection and nucleate boiling and F and S are the correction factors for each component. The following correlations by Dittus and Boelter [23] and Foster and Zuber [24] are used for h_{FC} and h_{NB}, respectively.

$$h_{FC} = 0.023 Re_L^{0.8} Pr_L^{0.4} \frac{k_L}{D} \tag{11}$$

$$h_{NB} = \frac{0.00122 k_L^{0.79} c_{pL}^{0.45} \rho_L^{0.49} \Delta T_W^{0.24} \Delta p_W^{0.75}}{\sigma^{0.5} \mu_L^{0.29} \Delta h_{VAP}^{0.24} \rho_V^{0.24}} \tag{12}$$

where Re_L is the single-phase flow Reynolds number ($= GD/\mu_L$), Pr is the Prandtl number, k is the thermal conductivity, D is the channel diameter, c_p is the specific heat at constant pressure, ΔT_W and Δp_W are the wall superheat and corresponding increase in the saturation pressure, σ is the surface tension, μ is the viscosity, and the subscript L denotes the liquid phase. Chen's correlation was originally developed to evaluate heat transfer rate in saturated flow boiling. When it is applied to subcooled flow boiling, F and S are often calculated by [19,25]

$$F = 1 \tag{13}$$

$$S = \frac{1}{1 + 2.53 \times 10^{-6} Re_L^{1.17}} \tag{14}$$

The nucleate boiling heat transfer q_{NB} may be partitioned into the components associated with vapor formation during nucleation q_{VAP} and pumping effect (micro convection of liquid induced by nucleation) q_{PUMP} [26,27].

$$q_{NB} = q_{VAP} + q_{PUMP} \tag{15}$$

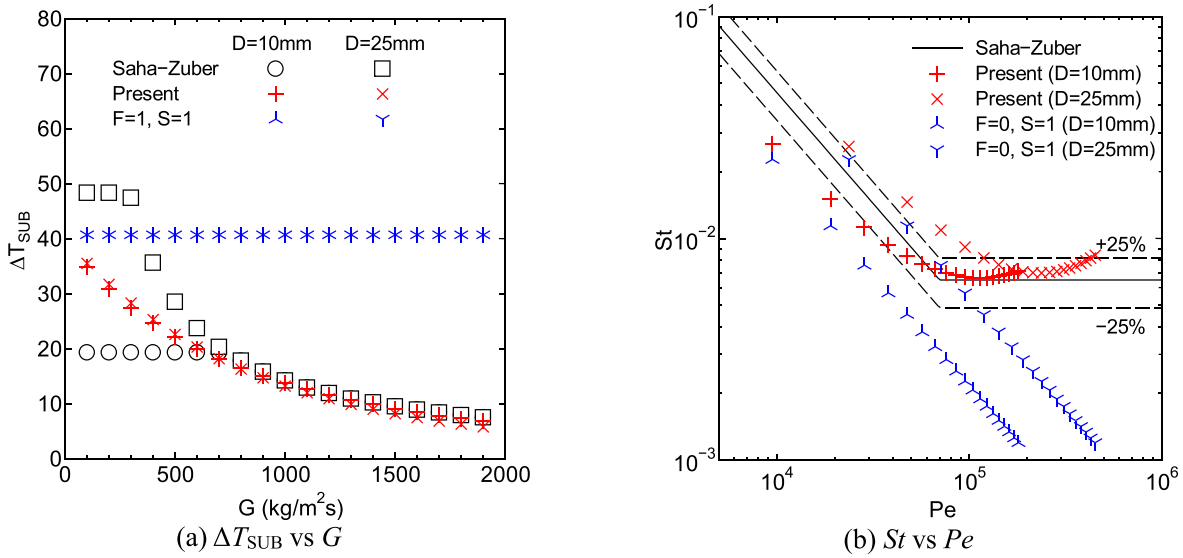

(a) ΔT_{SUB} vs G (b) St vs Pe

Fig. 4. Effect of flow channel diameter on the calculated OSV condition.

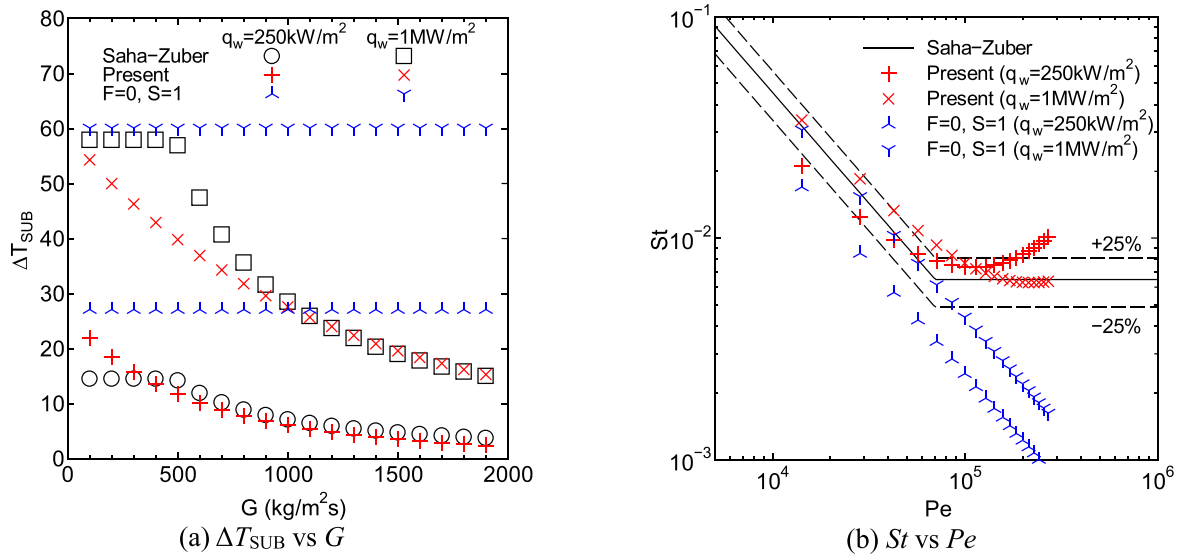

(a) ΔT_{SUB} vs G (b) St vs Pe

Fig. 5. Effect of heat flux on the calculated OSV condition.

Assuming that the subcooled liquid pumped to the heated wall is proportional in volume to the produced vapor bubbles and heated to the saturation temperature, one obtains

$$\frac{q_{PUMP}}{\rho_L c_{pL} \Delta T_{SUB}} = C_3 \frac{q_{VAP}}{\rho_V \Delta h_{VAP}} \tag{16}$$

where C_3 is the model constant. Eliminating q_{PUMP} using Eqs. (15) and (16), q_{VAP} is expressed by

$$q_{VAP} = \frac{q_{NB}}{1 + C_3 \rho^* \Delta\theta_{SUB}} \tag{17}$$

where ρ^* is the density ratio ($= \rho_L/\rho_V$) and $\Delta\theta_{SUB}$ is the dimensionless liquid subcooling ($= c_{pL}\Delta T_{SUB}/\Delta h_{VAP}$).

Substituting Eqs. (10) and (17) to Eq. (7), the following relation is satisfied at OSV.

$$\alpha_C = \frac{h^* \Delta\theta_W}{C_1 C_2 \Delta\theta_{SUB}(1 + C_3 \rho^* \Delta\theta_{SUB})} \tag{18}$$

where $\Delta\theta_W$ is the dimensionless wall superheat ($= c_{pL}\Delta T_W/\Delta h_{VAP}$) and h^* is the heat transfer coefficient ratio ($= Sh_{NB}/h_{CON}$). Solving the above equation for $\Delta\theta_{SUB}$, the dimensionless liquid subcooling at OSV is calculated by

$$\Delta\theta_{SUB} = -\frac{1}{2C_3\rho^*} + \sqrt{\left(\frac{1}{2C_3\rho^*}\right)^2 + \frac{h^*\Delta\theta_W}{\alpha_C C_1 C_2 C_3 \rho^*}} \tag{19}$$

To calculate the critical subcooling at POSV using Eq. (19), the condensation heat transfer coefficient h_{CON}, the bubble size d_b, and the bubble velocity relative to liquid u_R must be known. For the condensation heat transfer coefficient h_{CON}, the following Ranz-Marshall correlation for sphere [23] is used.

$$h_{CON} = 2 + 0.6 Re_B^{0.5} Pr_L^{0.33} \frac{k_L}{d_B} \tag{20}$$

where Re_B is the bubble Reynolds number ($= \rho_L u_R d_B/\mu_L$), d_B is the bubble diameter, and u_R is the bubble velocity relative to liquid. It is known that dependencies of bubble size on thermal-hydraulic parameters are extremely complex in subcooled flow boiling [28]. In this work, as the simplest method to calculate d_B, the Bond

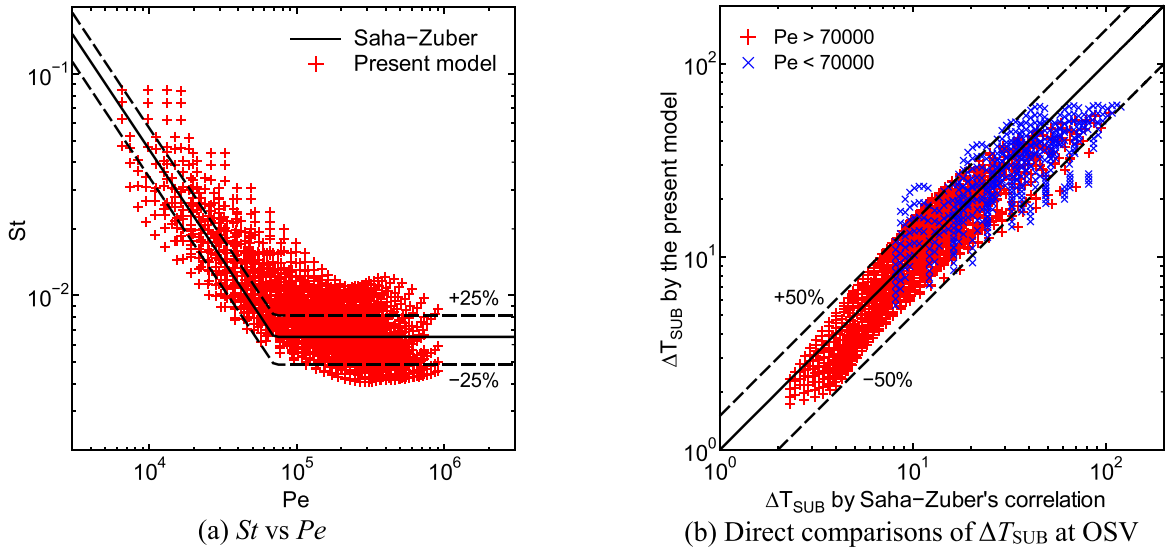

Fig. 6. Comparisons of the OSV conditions calculated by the present and Saha-Zuber correlations.

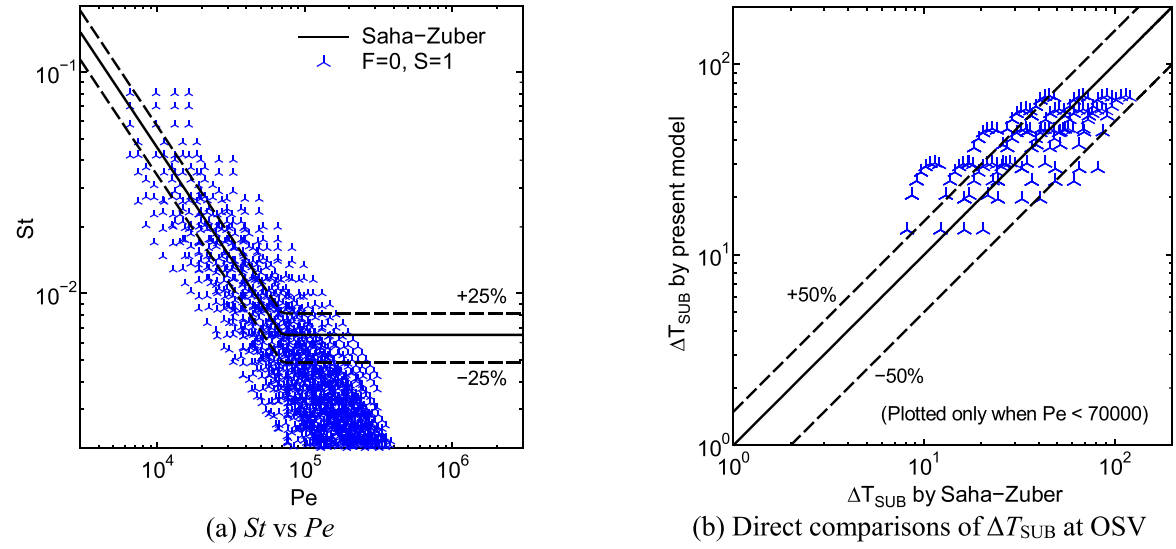

Fig. 7. Comparisons of the OSV conditions calculated by the present and Saha-Zuber correlations under the setting of $F = 0$ and $S = 1$.

number ($= g\Delta\rho {d_B}^2/\sigma$) is assumed constant [29].

$$d_B = C_4\sqrt{\frac{\sigma}{g\Delta\rho}} \tag{21}$$

where C_4 is the model constant and $\Delta\rho$ refers the density difference between the phases ($= \rho_L - \rho_V$). Using the drag coefficient C_D, the relative velocity u_R is expressed by

$$u_R = \sqrt{\frac{4\Delta\rho g d_B}{3C_D\rho_L}} \tag{22}$$

The following correlation by Ishii and Chawla [30] can be used to estimate C_D.

$$C_D = \max\left[\frac{24}{Re_B}(1 + 0.1Re_B^{0.75}),\ \min\left\{\frac{2}{3}\sqrt{Eo},\ \frac{8}{3}\right\}\right] \tag{23}$$

where Re_B is the bubble Reynolds number ($= \rho_L u_R d_B/\mu_L$) and Eo is the Eötvös number ($= g\Delta\rho {d_B}^2/\sigma$).

3. Prediction capability of the present OSV model

3.1. Comparison with Saha and Zuber's correlation

To test the prediction capability of the present model, the calculated values of ΔT_{SUB} at POSV are compared with those calculated by the following Saha and Zuber's correlation [9].

$$\Delta T_{SUB} = \min\left[\frac{q_W D}{455k_L},\ \frac{q_W}{0.0065Gc_{pL}}\right] \tag{24}$$

The above equation predicts that ΔT_{SUB} at POSV does not depend on G at low mass fluxes and decreases in inverse proportion to G at high mass fluxes. This is the main reason why Saha and Zuber called the low and high mass flux regions as the thermally and hydrodynamically controlled regions, respectively. Using the Stanton number ($St = q_W/Gc_{pL}\Delta T_{SUB}$) and the Peclet number ($Pe = GDc_{pL}/k_L$), Eq. (24) is rewritten in the dimensionless form as

$$St = \max\left[\frac{455}{Pe},\ 0.0065\right] \tag{25}$$

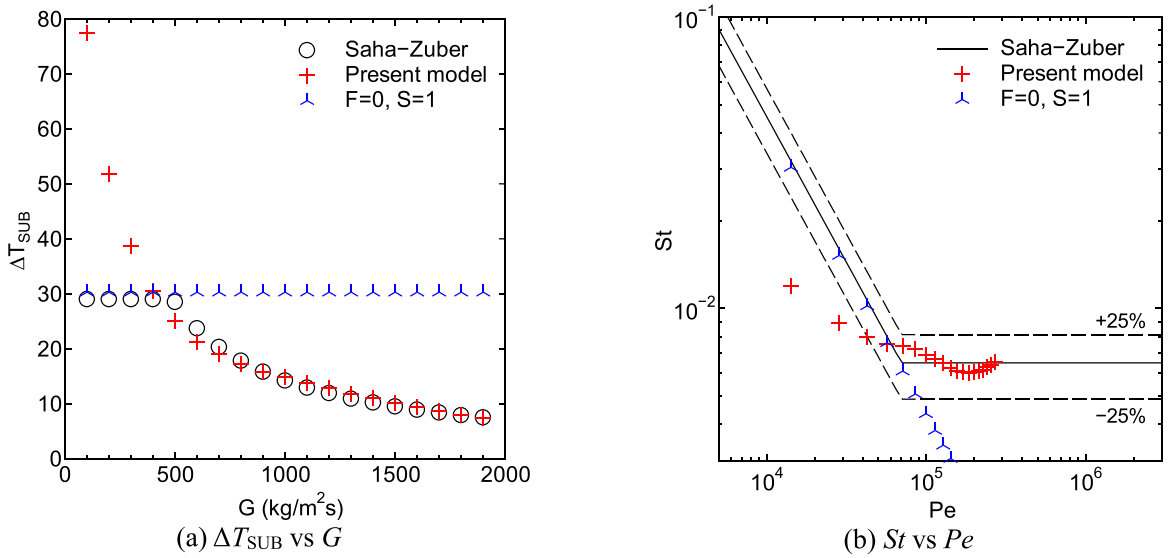

(a) ΔT_{SUB} vs G (b) St vs Pe

Fig. 8. Comparisons of the values of ΔT_{SUB} at OSV calculated by the present and Saha-Zuber correlations in the standard conditions of P, D and q_W when C_3 was corrected.

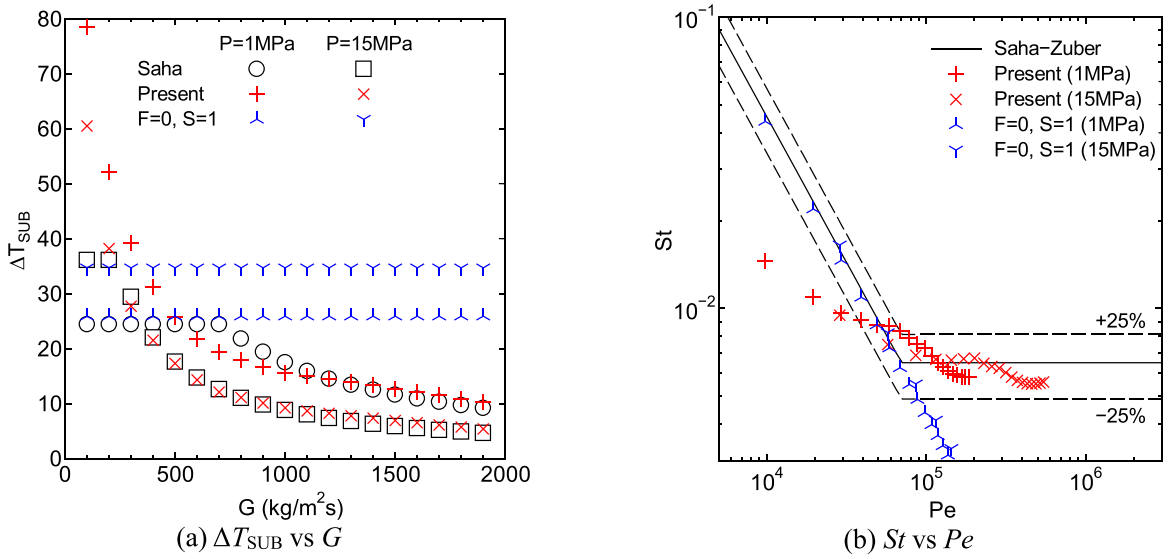

(a) ΔT_{SUB} vs G (b) St vs Pe

Fig. 9. Effect of pressure on the calculated OSV condition when C_3 was corrected.

From the intersection of the two correlations, the boundary between the thermally and hydrodynamically controlled regions is defined by $Pe = 70{,}000$.

In the comparison, to explore the basic predictive performance of the present model, the most fundamental values were used for the model constants:

$$\alpha_C = 0.3 \tag{26}$$

$$C_1 = C_2 = C_3 = C_4 = 1 \tag{27}$$

Here, the value of α_C was determined from the available knowledge on the flow regime transition from bubbly flow to slug flow in gas-liquid two-phase flow [19,21]. Referring the normal operation condition in BWR, the standard values of the analytical parameters and their ranges were set as shown in Table 1.

Fig. 2 displays the comparisons of the values of ΔT_{SUB} at POSV calculated by the present model and Saha-Zuber correlation when P, D and q_W were set at the standard values and G was varied within 100−1900 kg/m^{2}s. The results are plotted on the ΔT_{SUB}−G and St−Pe diagrams in Fig. 2(a) and (b), respectively. The calculated results when the values of F and S used in Chen's correlation were set to 0 and 1, respectively, are also presented with the blue symbols in these figures, that will be discussed later. Fig. 2(a) demonstrates that the present mechanistic model (red symbols) succeeds to express the overall decreasing trend of ΔT_{SUB} with an increase in G suggested by Saha and Zuber's correlation (black symbols). It should however be noted that independency of ΔT_{SUB} on G in the low mass flux range is not reproduced at all. In addition, in the hydrodynamically controlled region, the slope pre-

Table 1
Parameter values in the standard condition.

Parameters	Standard value	Range
P	7 MPa	1−15 MPa
D	15 mm	10−25 mm
q_W	500 kW/m^2	250−1000 kW/m^2
G	1000 kg/m^{2}s	100−1900 kg/m^{2}s

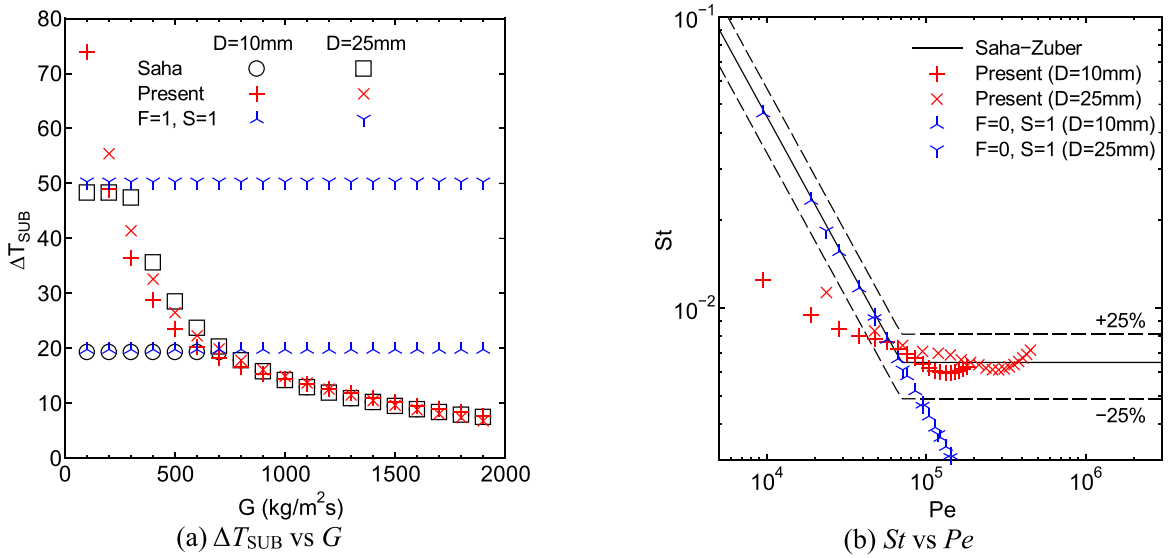

(a) ΔT_{SUB} vs G (b) St vs Pe

Fig. 10. Effect of flow channel diameter on the calculated OSV condition when C_3 was corrected.

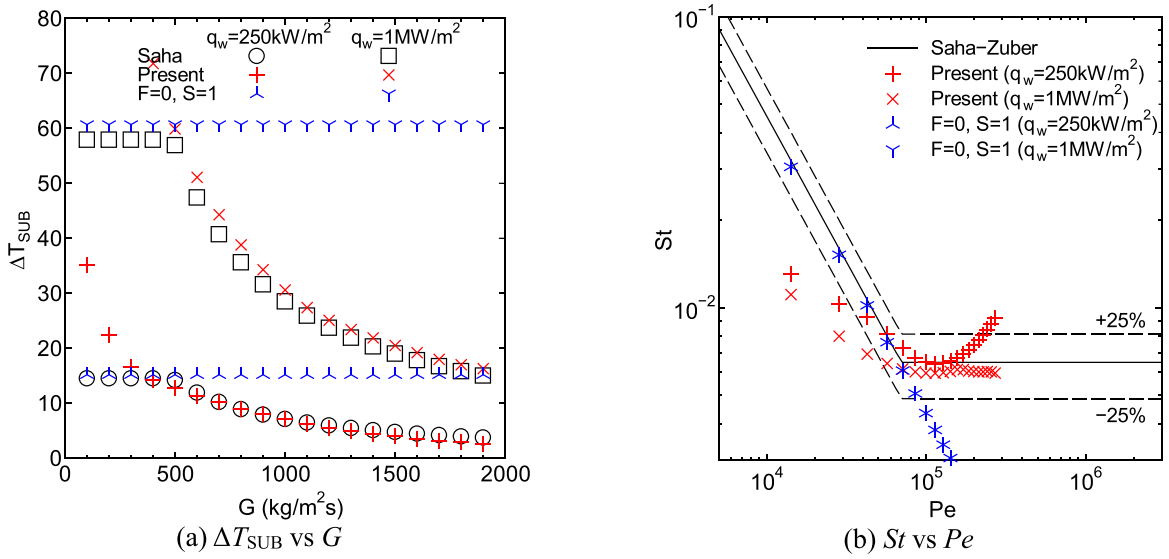

(a) ΔT_{SUB} vs G (b) St vs Pe

Fig. 11. Effect of heat flux on the calculated OSV condition when C_3 was corrected.

dicted by the present model is gentler within 500−1100 kg/m^{2}s and steeper within 1100−1900 kg/m^{2}s, with the result that the Stanton number is not constant in the range of $Pe > 70{,}000$ in Fig. 2(b). Figs. 3−5 represent the results when the values of P, D and q_W were changed. The values of ΔT_{SUB} calculated by the present model and Saha-Zuber correlation are in the same order of magnitude in all the analytical conditions, showing that the proposed OSV mechanism described in the preceding section is plausible. Distinct disagreement is however seen in the hydrodynamically controlled region in Fig. 3. The present model tends to underestimate ΔT_{SUB} as the pressure rises.

The OSV conditions in all the analytical conditions calculated by the present and Saha-Zuber correlations are compared in Fig. 6(a) and (b). Fig. 6(a) represents that although scattering is noticeable, the decreasing trend of St with an increase in Pe in the thermally controlled region and the independency of St on Pe in the hydrodynamically region are reproduced by the present model fairly well. In consequence, the values of ΔT_{SUB} calculated by the two correlations coincide with each other within the error range of about ±50% in Fig. 6(b). It can also be seen in Fig. 6(a) and (b) that the disagreement is slightly greater in the thermally controlled region of $Pe < 70{,}000$ since the dependency of ΔT_{SUB} on G is different between the two correlations.

3.2. Modification in the thermally controlled region

Saha and Zuber's correlation suggest that the OSV condition is not influenced by G in the thermally controlled region of $Pe < 70{,}000$ but this trend is not reproduced by the present model. It can be seen in Eq. (19) that in the present model, the effect of G on ΔT_{SUB} at POSV is considered only through ΔT_W, implying that the effect of G disappears if the wall heat transfer is not influenced by G. This situation can be realized if the two parameters used in Chen's correlation are set as $F = 0$ and $S = 1$. Under this setting, the wall heat transfer in subcooled flow boiling is assumed identical to the nucleate boiling heat transfer in pool boiling. Validity of this setting might be supported by the fact that the heat transfer in nucleate pool boiling is largely independent of the liquid subcool-

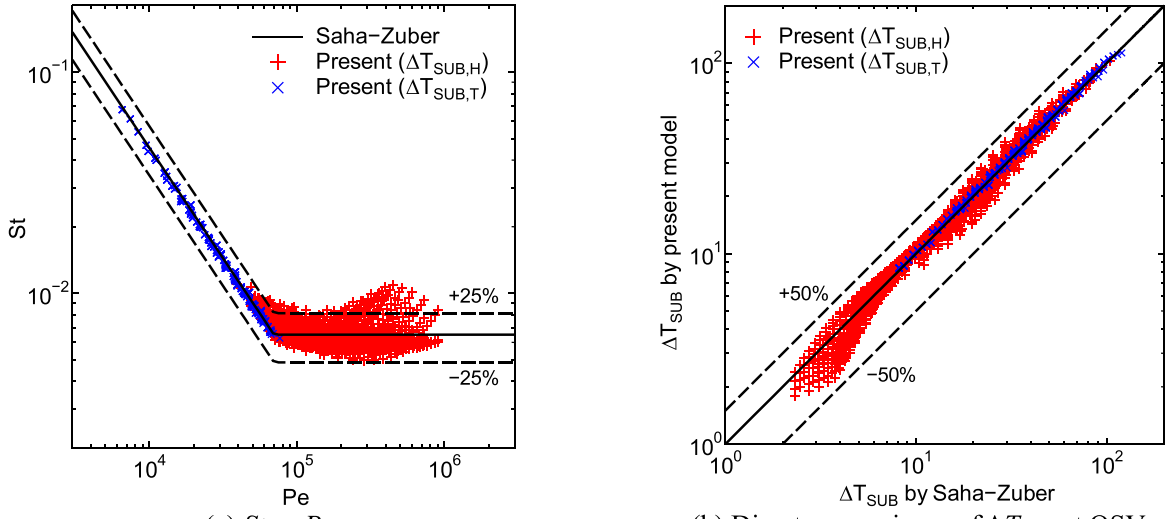

(a) St vs Pe (b) Direct comparisons of ΔT_{SUB} at OSV

Fig. 12. Comparisons of the OSV conditions calculated by the present and Saha-Zuber correlations when C_3 was corrected.

ing [29]. It is therefore assumed that the forced convective flow of subcooled liquid has no net influence on the wall heat transfer at low mass fluxes. The calculated OSV conditions under the settings of $F = 0$ and $S = 1$ are presented in Figs. 2–5 with the blue symbols. It can be confirmed that the effect of G is eliminated under these settings. As for the effects of other parameters, the present model succeeds to reproduce the increasing trends of ΔT_{SUB} with increased values of P and q_W (Figs. 3 and 5) but fails to express the obvious effect of D in the thermally controlled region (Fig. 4). A possible reason of this failure is the elimination of the channel diameter effect on the bubbles size. Assuming that the boundary layer thickness and consequently the bubble size d_B tend to increase with an increase in D, the condensation heat transfer coefficient h_{CON} decreases with an increase in D (see Eq. (20)). This leads to an increase in h^* and consequently increases in $\Delta\theta_{SUB}$ and ΔT_{SUB} (see Eq. (19)).

The calculated OSV conditions under the setting of $F = 0$ and $S = 1$ are compared with the Saha-Zuber correlation in Fig. 7(a) and (b) where the results are plotted only when $Pe < 70{,}000$ in Fig. 7(b) since Fig. 7(a) indicates clearly that this setting should not be applied to the hydrodynamically controlled region of $Pe > 70{,}000$. Although the agreement of the calculated values of ΔT_{SUB} with Saha and Zuber's correlation shown in Fig. 7(b) is similar to the original model (see Fig. 6(b)), Fig. 7(a) shows that the inverse proportion of St to Pe in the thermally controlled region suggested by Saha and Zuber is reproduced well by the simple modification described above.

3.3. Correction of the model constants

The fairly good agreements with Saha and Zuber's correlation presented in the previous sections suggest strongly that the onset of significant void in subcooled flow boiling is induced by the global bubble coalescence commenced when the bubble layer void fraction reaches the critical value. Since the agreement was however still unsatisfactory, it is attempted in this section that the model constants are adjusted so as to achieve better agreement. Obviously, the prediction capability of the present model never surpasses that of Saha and Zuber's correlation by this adjustment. Sufficiently good agreement with Saha and Zuber's correlation would however be necessary since their correlation is known to show good agreement with the experimental data accumulated in wide range of thermal-hydraulic conditions [4,9,10]. It is also noted that since the present correlation was developed mechanistically, it may be useful to estimate the change of the OSV condition when the situation deviates from that tested in ordinary experiments; several examples are the effects of rapid transient, nonfully developed velocity profile, and complicated cross-sectional geometry of flow channel. In exploring the OSV condition in such more complicated situations, good prediction capability under fundamental conditions is desired.

Mainly due to extreme complexity of the elementary processes encountered in subcooled flow boiling, the present model contains many unknown factors. Particularly important ones are the critical void fraction α_C for the global bubble coalescence to occur and the four model constants C_1 to C_4 regarding the heat transfer area of condensation, the liquid subcooling in the bubble layer, the liquid volume pumped to the heated wall by nucleation, and the bubble size, respectively. In addition, Chen's correlation for the wall heat transfer should also contain error to some extent [22] and it is not obvious if Ranz and Marshall's correlation for the condensation heat transfer coefficient and Ishii and Chawla's correlation for the drag coefficient can be applied without change to the bubbles that are present in close proximity to the heated wall in subcooled flow boiling. Since adjusting all these factors is practically not possible, the model constant C_3 was selected as the tuning parameter to achieve better agreement. C_3 was selected because this parameter was introduced to express the volume ratio of the pumped liquid to a nucleated bubble on the heated wall and its value was supposed most uncertain.

The analytical parameters used in this work are the pressure P, flow channel diameter D, heat flux q_W and mass flux G. To explore the effects of these four parameters on the OSV condition, the following four dimensionless numbers were selected.

$$\rho^* = \frac{\rho_L}{\rho_V} \tag{28}$$

$$D^* = \frac{D}{d_B} \tag{29}$$

$$q^* = \frac{\rho_L q_W d_B}{\rho_V \Delta h_{VAP} \mu_L} \tag{30}$$

$$G^* = \frac{G \Delta h_{VAP}}{q_W} \left(\frac{\rho_V}{\rho_L}\right)^n \tag{31}$$

where ρ^* is the density ratio of liquid to vapor, D^* is the diameter ratio of flow channel to bubbles, q^* is the dimensionless heat flux (the Reynolds number of the micro convection of liquid induced around the growing bubble when d_B and $q_W/\rho_V\Delta h_{VAP}$ are used as the characteristic length and velocity scales, respectively), and G^* is the parameter related to the inertia ratio of the inlet mass flux to the micro convection. It was further assumed that C_3 is expressed in the form

$$C_3 = f_1(\rho^*)f_2(D^*)f_3(q^*)f_4(G^*) \tag{32}$$

After many trials, it was found the following equations are satisfactory to achieve good agreement with Saha and Zuber's correlation. First, for the hydrodynamically controlled region where the values of F and S are calculated by Eqs. (13) and (14), the suggested functions are

$$f_1(\rho^*) = \max\left[67(\rho^*)^{-1.5},\ 1.6(\rho^*)^{-0.38}\right] \tag{33}$$

$$f_2(D^*) = 1.8(D^*)^{-0.39} \tag{34}$$

$$f_3(q^*) = 1 \tag{35}$$

$$f_4(G^*) = \min\left[1.5,\ \min\{2.6\times10^{-5}(G^*)^{1.6},\ 1.7\times10^{5}(G^*)^{-1.6}\}\right] \tag{36}$$

where the exponent n in Eq. (31) was set to 0.2. Next, for the thermally controlled region where $F = 0$ and $S = 1$,

$$f_1(\rho^*) = \min\left[1,\ 2.6(\rho^*)^{-0.25}\right] \tag{37}$$

$$f_2(D^*) = 330(D^*)^{-2.3} \tag{38}$$

$$f_3(q^*) = 120(q^*)^{-1.0} \tag{39}$$

$$f_4(G^*) = 1 \tag{40}$$

The calculated OSV conditions after correcting C_3 are compared with Saha and Zuber's correlation in Figs. 8–11 in the same manner as in Figs. 2–5. Comparisons of Figs. 8−11 with Figs. 2–5 show that the agreement is improved substantially after correcting C_3.

As the roles of the four dimensionless quantities, the following qualitative discussions can be done. First, the suggested value of C_3 tends to decrease with an increase in ρ^* in Eqs. (33) and (37). This may reflect the fact that the volume ratio of liquid pumped to the heated wall decreases as the liquid becomes heavier than vapor. Second, if the bubble is much smaller than the channel diameter, the bubble is entirely contained in the thermal boundary layer near the wall and it would be difficult to convey the cold bulk liquid to the heated wall by the nucleation-induced micro convection. This may be presumed as the reason why C_3 tends to decrease with an increase in D^* in Eqs. (34) and (38). Third, by analogy with the boundary layer thickness in the case of fluid flow over the flat plate [23], the liquid volume influenced by nucleation would be greater when the Reynolds number of the liquid flow induced by nucleation is lower. This tendency is consistent with Eq. (39) that suggests that the pumping effect is suppressed with an increase in q^*. As for the effect of G^* in Eq. (36), no plausible explanation can be done and it should be regarded as a fully empirical relation just to improve the agreement with Saha and Zuber's correlation.

From the results of comparison displayed in Figs. 8–11, the present model can predict the critical liquid subcooling at OSV by

$$\Delta T_{SUB} = \min(\Delta T_{SUB,H},\ \Delta T_{SUB,T}) \tag{41}$$

where $\Delta T_{SUB,H}$ and $\Delta T_{SUB,T}$ refer the critical liquid subcoolings calculated by the models for the hydrodynamically and thermally controlled regions, respectively. The results of comparison for all the analytical conditions are presented in Fig. 12. Comparing these results with those in Fig. 6, it can be seen that the agreement is improved substantially by the correction of C_3.

4. Conclusions

Theoretical investigations were carried out to develop a mechanistic model for the criterion to cause the onset of significant void in subcooled flow boiling. Main conclusions of this work are summarized as follows.

(1) Based on the available knowledge on the flow regime transition in gas-liquid two-phase flow, it was postulated that global bubble coalescence occurs when the bubble layer void faction near the heated wall reaches the critical value. It was supposed that this phenomenon causes the onset of significant void (OSV) since the bubble interfacial area and consequently the condensation rate decrease substantially. It was shown that the OSV conditions calculated on this hypothesis are in fairly good agreement with those calculated using the widely-accepted OSV correlation by Saha and Zuber. It should be noted that although the supposed mechanism of OSV was simple, considerable simplifications were necessary to calculate the OSV condition due to extreme complexity of the phenomena encountered in subcooled flow boiling. The fairly good agreement with Saha and Zuber's correlation would be regarded as the evidence showing that the constitutive models as well as the base mechanism of OSV utilized in this work are plausible.

(2) Empirical correlations were developed for the model constant regarding the liquid volume pumped to the heated surface by nucleation. Agreement with Saha and Zuber's correlation was improved substantially by using these correlations. It is commonly recognized that empirical correlations should not be used in the thermal-hydraulic conditions beyond the range of the base data used in the development but mechanistic models can be extended to such conditions provided the mechanism is unchanged. Hence, although the prediction capability of the proposed model does not surpass that of Saha and Zuber's correlation in simple situations, the present model is expected advantageous to explore the OSV condition in complex situations since it was derived mechanistically based on the thermal-hydraulic phenomena encountered in subcooled flow boiling.

Author statement

Tomio Okawa: Conceptualization, Methodology, Validation, Formal analysis, Investigation, Project administration, Writing - Original Draft, Writing - Review & Editing

Declaration of Competing Interest

None.

CRediT authorship contribution statement

Tomio Okawa: Conceptualization, Methodology, Validation, Formal analysis, Investigation, Project administration, Writing – original draft, Writing – review & editing.

Acknowledgments

The authors wish to thank Dr. Naofumi Tsukamoto (Nuclear Regulation Authority) for his insightful comments on this work.

The present study includes the results obtained in the project of "Elucidation of the boiling characteristics in the subcooled flow boiling at low pressures" entrusted by Nuclear Regulation Authority in 2020.

References

[1] J.G. Collier, J.R. Thome, Convective Boiling and Condensation, 3rd ed., Clarendon Press, Oxford, 1994 Chap. 6.
[2] R.T. Lahey Jr., F.J. Moody, The Thermal-Hydraulics of a Boiling Water Nuclear Reactor, 2nd ed., American Nuclear Society, Illinois, 1993 Sec. 5.3.2.
[3] S.G. Kandlikar, Subcooled flow boiling, in: S.G. Kandlikar, M. Shoji, V.K. Dhir (Eds.), Handbook of Phase Change, Taylor & Francis, 1999 Sec. 15.2.
[4] C. Cai, I. Mudawar, H. Liu, X. Xi, Assessment of void fraction models and correlations for subcooled boiling in vertical upflow in a circular tube, Int. J. Heat Mass Transfer 171 (2021) 121060.
[5] P. Griffith, J.A. Clark, W.M. Rohsenow, Void volumes in subcooled boiling systems, ASME Paper 58-HT-19, U.S. National Heat Transfer Conference, 1958.
[6] R.W. Bowring, Physical Model Based on Bubble Detachment and Calculations of Steam Voidage in the Subcooled Region of a Heated Channel, OECD Halden Reactor Project, 1962 Report HPR-10.
[7] S.Y. Ahmad, Axial distribution of bulk temperature and void fraction in a heated channel with inlet subcooling, ASME J. Heat Transfer 92 (1970) 595–609.
[8] K. Sekoguchi, O. Tanaka, S. Esaki, T. Imasaka, Prediction of void fraction in subcooled and low quality boiling regions, Bull. JSME 23 (1980) 1475–1482.
[9] P. Saha, N. Zuber, Point of net vapor generation and vapor void fraction in subcooled boiling, in: Proceedings of the 5th International Heat Transfer Conference, Tokyo, 1974, pp. 175–179.
[10] S.C. Lee, S.G. Bankoff, A comparison of predictive models for the onset of significant void at low pressures in forced-convection subcooled boiling, J. Mech. Sci. Technol. 12 (3) (1998) 504–513.
[11] S. Levy, Forced convection subcooled boiling prediction of vapor volumetric fraction, Int. J. Heat Mass Transfer 10 (7) (1967) 951–965.
[12] G.E. Dix, Vapor Void Fractions for Forced Convection with Subcooled Boiling at Low Flow Rates Ph.D. Thesis,, University of California, 1971.
[13] E.L. Bibeau, M. Salcudean, A study of bubble ebullition in forced-convective subcooled nucleate boiling at low pressures, Int. J. Heat Mass Transfer 37 (15) (1994) 2245–2259.
[14] O.M. Zeitoun, Subcooled Flow Boiling and Condensation PhD Thesis, McMaster University, Hamilton, ON, 1994.
[15] R. Ahmadi, T. Ueno, T. Okawa, Bubble dynamics at boiling incipience in subcooled upward flow boiling, Int. J. Heat Mass Transfer 55 (1–3) (2012) 488–497.
[16] Q. Sun, R. Yang, H. Zhao, Predictive study of the incipient point of net vapor generation in low-flow subcooled boiling, Nucl. Eng. Des. 225 (2003) 249–256.
[17] I. Kataoka, S. Kodama, A. Tomiyama, A. Serizawa, Study on analytical prediction of forced convective CHF based on multi-fluid model, Nucl. Eng. Des. 175 (1997) 107–117.
[18] T.-W. Ha, B.-J. Yun, J.J. Jeong, Improvement of the subcooled boiling model for thermal–hydraulic system codes, Nucl. Eng. Des. 364 (2020) 110641.
[19] P.B. Whalley, Boiling, Condensation, and Gas-Liquid Flow, Clarendon Press, Oxford, 1987 Chap. 2.
[20] J.A. Trapp, G.A. Mortensen, A discrete particle model for bubble-slug two-phase flows, J. Comput. Phys. 107 (2) (1993) 367–377.
[21] K. Mishima, M. Ishii, Flow regime transition criteria for upward two-phase flow in vertical tubes, Int. J. Heat Mass Transfer 27 (5) (1984) 723–737.
[22] J.C. Chen, Correlation for boiling heat transfer to saturated fluids in convective flow, Ind. Eng. Chem. Process Des. Dev. 5 (3) (1966) 322–329.
[23] F.P. Incropera, D.P. DeWitt, A. Lavine, T.L. Bergman, Fundamentals of Heat and Mass Transfer, 6th ed., Willey, New York, 2006.
[24] H.K. Forster, N. Zuber, Dynamics of vapor bubbles and boiling heat transfer, AIChE J. 1 (4) (1955) 531–535.
[25] J. Yan, Q. Bi, Z. Liu, G. Zhu, L. Cai, Subcooled flow boiling heat transfer of water in a circular tube under high heat fluxes and high mass fluxes, Fusion Eng. Des. 100 (2015) 406–418.
[26] N. Kurul, M.Z. Podowski, Multidimensional effects in forced convection subcooled boiling, in: Proceedings of the 9th International Heat Transfer Conference, Jerusalem, Israel, 2020, pp. 21–26.
[27] N. Basu, G.R. Warrier, V.K. Dhir, Wall heat flux partitioning during subcooled flow boiling: part 1 - model development, J. Heat Transfer 127 (2) (2005) 131–140.
[28] M. Conde-Fontenla, C. Paz, M. Concheiro, G. Ribatski, On the width and mean value of bubble size distributions under subcooled flow boiling, Exp. Therm. Fluid Sci. 124 (2021) 110368.
[29] V.P. Carey, Liquid-Vapor Phase-Change Phenomena, 2nd ed., CRC Press, New York, 2008.
[30] M. Ishii, T.C. Chawla, Local Drag Laws in Dispersed Two-Phase Flow, Argonne National Laboratory Report, 1979 ANL-79-105.